Diffusion mechanisms for silicon di-interstitials

Yaojun A. Du,* Richard G. Hennig, and John W. Wilkins
Department of Physics, Ohio State University, Columbus, Ohio 43210, USA
(Received 6 October 2005; revised manuscript received 4 May 2006; published 12 June 2006)

Tight-binding molecular dynamics and density-functional simulations on silicon seeded with a di-interstitial reveal its detailed diffusion mechanisms. The lowest-energy di-interstitial performs a translation/rotation diffusion-step with a barrier of 0.3 eV and a prefactor of 11 THz followed by a reorientation diffusion step with a 90 meV barrier and a 2300 THz prefactor. The intermediate reorientation steps allow di-interstitials to diffuse isotropically along all possible ⟨111⟩ bond directions in the diamond lattice. The dominating diffusion barrier of 0.3 eV is not inconsistent with the experimental value of 0.6±0.2 eV. In addition, this lowest energy di-interstitial may diffuse to neighboring sites through an intermediate structure which is the bound state of two single interstitials. The process in which migrating single interstitials combine into a di-interstitial is exothermic with almost zero energy barrier.

DOI: 10.1103/PhysRevB.73.245203 PACS number(s): 61.72.Ji, 66.30.Lw, 71.15.Mb, 71.15.Pd

I. INTRODUCTION

Defects in the semiconductor can limit the performance of electronic devices. The simulation of semiconductor devices requires accurate defect properties. In the silicon manufacturing process, the ion-implantation induced interstitials can precipitate into extended {311} defects.[1] Despite considerable efforts, the nucleation and growth of these extended structures are not completely understood.[2–4] On the other hand, the growth from single interstitials to the extended structures is a multistep process. In this work we study the first step of that process, the diffusion of di-interstitials, and their formation from single interstitials in silicon.

Electron paramagnetic resonance (EPR) experiments have associated the so-called *P*6 center with a di-interstitial defect in crystalline silicon.[5,6] Applying uniaxial stress on neutron-, proton- or ion-implanted silicon, Lee[5,6] attributes the EPR *P*6 center to a di-interstitial aligned close to the ⟨001⟩ direction. An activation energy of 0.6±0.2 eV is extracted from the motion of the *P*6 center under an external uniaxial stress at temperatures of 370 and 344 K, respectively.[5] The low activation barrier indicates that this di-interstitial is highly mobile. However, the exact atomic configurations of di-interstitials and associated diffusion paths cannot be resolved experimentally due to their small size.[7] The revelation of the dynamics of di-interstitials relies on numerical simulations.

Based on density-functional calculations, Kim *et al.*[8] proposed a structure, I_2^a, for the di-interstitial defect in silicon and related its C_{1h} symmetry and the estimated 0.5 eV diffusion barrier to the experimental results for the *P*6 center. Moreover, Kim's results indicate that the I_2^a diffuses via a reorientation mechanism.[8] The I_2^a structure is believed to be the lowest-energy di-interstitial. Earlier molecular dynamics (MD) simulations by Gilmer *et al.*[9] with a classical potential[10] estimated an activation energy of 0.2 eV for di-interstitials. Posselt *et al.*[11] show that the motion of di-interstitials within a {110} plane could result in this low activation energy of 0.2 eV. Recently, Cogoni *et al.*[12] calculated an activation barrier of 0.89 eV for di-interstitials by temperature-accelerated molecular-dynamics simulations[13] with the Kwon *et al.*[14] tight-binding (TB) potential. Their results suggest a given di-interstitial can hop along three of the six possible ⟨110⟩ directions.[12] Hence, previous theoretical works conflict in both diffusion mechanism and diffusion barrier for di-interstitials.

This work addresses the conflicts between previous work by examining several plausible diffusion pathways. The diffusion mechanism of the compact tri-interstitial[15] inspires an initial path for the diffusion mechanism of the I_2^a di-interstitials. Nudged-elastic band (NEB) calculations[16,17] using density functional methods[18–20] refine the transition path and determine the diffusion barriers of the path connecting the three lowest energy di-interstitial structures found in previous tight-binding molecular dynamics simulations.[2] Harmonic transition state theory[21] determines the diffusion rates. The calculations are performed with the Vienna AB-INITIO Simulation Package (VASP).[18,19] Details of the methods[22] are described in our previous work[15] on the diffusion mechanism of tri-interstitial defects in silicon.

We find that the di-interstitial ground state structure I_2^a can diffuse back and forth to a neighboring site with a diffusion barrier of 0.3 eV and can reorient with a barrier of only 0.09 eV such that the di-interstitials can perform a translation/rotation along all four possible ⟨111⟩ bond directions in the diamond lattice with intermediate reorientation steps. The formation of I_2^a from two single interstitials is strongly exothermic with a negligible energy barrier and the capture radius between two single interstitials is about 3.2 Å.

II. THREE LOWEST-ENERGY DI-INTERSTITIALS

Richie *et al.*[2] studied the dynamics of di-interstitials and identified the three lowest-energy di-interstitials I_2^a, I_2^b, and I_2^c in tight-binding molecular dynamics (TB-MD) simulations for 64+2 atom cells. Verified by density-functional relaxations within 216+2 atom supercells, the I_2^a structure is the ground state di-interstitial with a formation energy of 2.83 eV/atom, and I_2^b and I_2^c are the excited state di-interstitial with formation energies of 3.23 eV/atom and 3.22 eV/atom, respectively.[2]

Figure 1 shows the results of the density of states calculations for the three di-interstitial structures I_2^a, I_2^b, and I_2^c

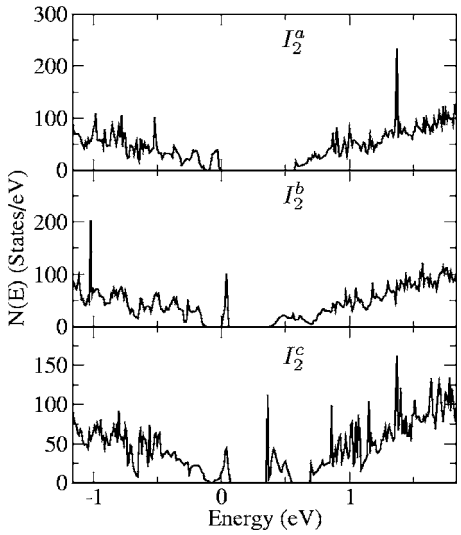

FIG. 1. The density of states (DOS) for the ground state di-interstitial I_2^a and excited state I_2^b and I_2^c. DOS are computed within 216+2 atom supercells. I_2^a exhibits a clear energy gap of 0.58 eV with no localized state. I_2^b has an occupied localized state in the energy gap while I_2^c has an unoccupied localized state in the energy gap.

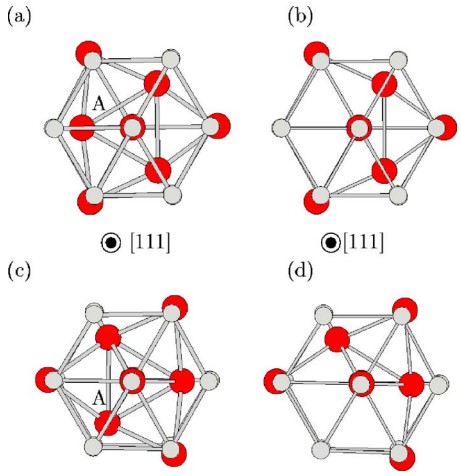

FIG. 2. (Color online) Two unrelaxed end points for the ground state di-interstitial, I_2^a, diffusion path constructed from two end points for the compact tri-interstitial, I_3^b, diffusion-path (Ref. 15). (a) The initial state for the I_3^b diffusion path. (b) The unrelaxed initial state for the I_2^a diffusion path constructed by removing atom A from (a). (c) The final state for the I_3^b diffusion path. (d) The unrelaxed final state for the I_2^a diffusion path constructed by removing atom A from (c). The structures shown in (a), (b), (c), and (d) are viewed along the [111] direction.

using 216+2 atom supercells. The I_2^a exhibits a clear energy gap of 0.58 eV compared to the energy gap of crystal silicon of 0.72 eV (Ref. 23) within the generalized gradient approximation[20] (GGA). The lack of localized states suggests that the neutral state may play a more significant role for the I_2^a structure and its diffusion than charged states. On the other hand, I_2^b has an occupied localized state in the energy gap while I_2^c has an unoccupied localized state in the energy gap. This indicates that positively and negatively charged states might play a relatively important role for I_2^b and I_2^c, respectively. In this work, we will exclusively study the diffusion and interconversion of three lowest-energy di-interstitials in the neutral charge state.

III. DIFFUSION PATHS OF THE GROUND STATE DI-INTERSTITIAL

Figure 2 demonstrates the similarity between the structure of the di-interstitial I_2^a and the compact tri-interstitial I_3^b.[15] The removal of one of the four interstitial atoms that form the tetrahedral defect I_3^b results in a structure that relaxes to I_2^a. Therefore, the tri-interstitial diffusion path[15] provides a possible pathway for the ground state di-interstitial I_2^a diffusion. We remove one of the three atoms of I_3^b, that is rotating and translating during the diffusion, from the initial and final state of the I_3^b diffusion-path (see Fig. 2) and relax the resulting structures to construct the end-point structures for a possible I_2^a diffusion path. The relaxations of the structures shown in Figs. 2(b) and 2(d) provide the initial and final state of the di-interstitial diffusion path shown in Fig. 3.

For the diffusion of the di-interstitial I_2^a structure the nudged-elastic band method[16,17] discovers a transition path consisting of two steps with another intermediate I_2^a structure. To accurately describe the diffusion path, we perform separate nudged-elastic band calculations for the two steps. Figure 3 shows the resulting pathway of the complete diffusion process. The diffusion path consists of: (1) a *translation/rotation* of the defect with a 0.3 eV barrier and a prefactor of 11 THz, followed by (2) a *reorientation* of the defect with a small energy barrier of 90 meV and a prefactor of 2300 THz. Starting from the intermediate structure in Fig. 3, the I_2^a can *either* perform a translation/rotation of atoms A and B (dumbbell AB) along $[\bar{1}1\bar{1}]$, *or* perform a translation/rotation of dumbbell BC and AC, along $[1\bar{1}\bar{1}]$ and $[\bar{1}\bar{1}1]$, respectively, after a corresponding reorientation step.

The translation/rotation step with a 0.3 eV barrier is dominated by the collective motion of the four atoms, A, B, C, and D in Fig. 3; all other atoms have displacements of less than 0.13 Å. Atoms C and D define an axis of rotation about which atoms A and B rotate, while all four atoms translate along the $\langle 111 \rangle$ direction defined by the vector $\overrightarrow{CD}$. The dumbbell of atoms A and B rotates 60° and the four atoms A, B, C, and D translate 0.68 Å along the $\langle 111 \rangle$ direction. The translation/rotation step of the I_2^a is the same pathway as found by Kim *et al.*[24]

Figure 4 represents the translation/rotation step of Fig. 3 by a two-dimensional plot of translation and rotation of the four most-displaced atoms, providing a further insight into the diffusion mechanism. The insets show the initial, saddle point and final state of the translation/rotation step viewed along the $\langle 111 \rangle$ direction and illustrate the concerted rotation of atoms A and B. The 2.29 Å bond length of the dumbbell AB remains nearly constant during the translation/rotation step. In Fig. 4 atoms A and B rotate counterclockwise from the initial to the final state. However, atoms A and B can also rotate clockwise from the initial state to another symmetry-related final state. Notably, the translation/rotation step alone

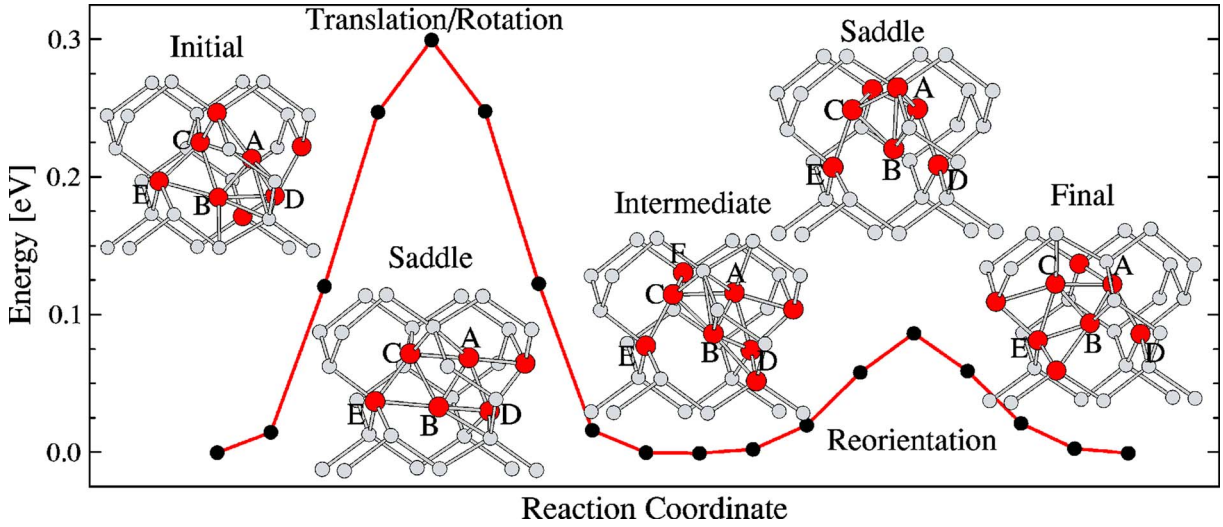

FIG. 3. (Color online) The diffusion pathway of the ground state di-interstitial I_2^a. The path consists of a combination of two steps, a translation/rotation and a reorientation. The translation/rotation step has an activation energy of 0.3 eV and a prefactor of 11 THz and the reorientation step has an activation energy of 90 meV and a prefactor of 2300 THz. The initial, intermediate and final structures are shown with the saddle point structures between them. During the translation/rotation, atoms C and D define an axis of rotation along the ⟨111⟩ direction about which atoms A and B are rotating; meanwhile, atoms A, B, C, and D translate along the ⟨111⟩ axis. Following the reorientation, atoms E and A define a new possible ⟨111⟩ axis of rotation and translation. The atoms B, C, E, and A in the final state are now equivalent to the atoms A, B, C, and D in the initial structure and can now perform another translation/rotation step. The intermediate I_2^a can *either* perform a translation/rotation step back along $[\bar{1}1\bar{1}]$, *or* perform a translation/rotation step along $[1\bar{1}\bar{1}]$ and $[\bar{1}\bar{1}1]$, respectively, after a corresponding reorientation step.

does not allow for the long-range diffusion of di-interstitials.

The reorientation step with a 90 meV barrier in Fig. 3 enables the long-range diffusion of di-interstitials by allowing for a translation/rotation step along another symmetry-related ⟨111⟩ direction. During the reorientation, atoms A, B, and C show displacements larger than 0.65 Å. All other atoms have displacements smaller than 0.35 Å. In Fig. 3 the intermediate I_2^a with the ⟨110⟩ split dumbbell defined by atoms A and B diffuses to the final I_2^a with the dumbbell defined by atoms B and C. Now the structure can perform another translation/rotation step following the ⟨111⟩ direction

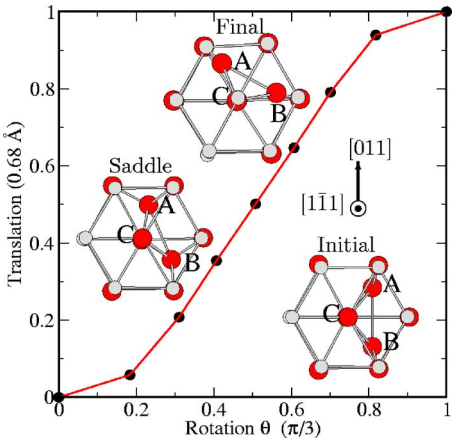

FIG. 4. (Color online) Translation/rotation path with seven images projected onto two-dimensional reduced coordinates. Inset: showing initial, saddle, final images along the transition path. The dumbbell AB rotates around $[1\bar{1}1]$ while translating along the $[1\bar{1}1]$ direction.

defined by atoms A and E. We compute a diffusion rate $\Gamma = 2300\ \text{THz}\exp(-0.09\ \text{eV}/k_BT)$ for the reorientation step, in contrast to the diffusion rate $\Gamma = 11\ \text{THz}\exp(-0.3\ \text{eV}/k_BT)$ for the translation/rotation step. The reorientation step occurs much more frequently than the translation/rotation. As a result, the overall diffusion of the di-interstitial is dominated by the translation/rotation step with a 0.3 eV barrier and a prefactor of 11 THz.

We show that any di-interstitial I_2^a can perform isotropic diffusion along all four ⟨111⟩ directions. Figure 3 illustrates the diffusion of the di-interstitial I_2^a structure by a translation/rotation step along one particular $[1\bar{1}1]$ direction defined by atoms C and D of the initial structure. In the intermediate structure of Fig. 3, atoms A and E and atoms B and F are related by reflection symmetry. The mirror plane contains atoms C and D and is perpendicular to the bond between atoms A and B. The intermediate I_2^a can now *either* (1) make a translation/rotation step of dumbbell AB back along the $[\bar{1}1\bar{1}]$ defined by atoms C and D, *or* (2) perform a reorientation then a translation/rotation step of dumbbell BC along the $[1\bar{1}\bar{1}]$ defined by atoms A and E, *or* (3) perform a reorientation then a translation/rotation step of dumbbell AC along the $[\bar{1}\bar{1}1]$ defined by atoms B and F. As shown in Fig. 4, during the translation/rotation step from the initial structure to the intermediate structure in Fig. 3, atoms A and B rotate counterclockwise. On the other hand, atoms A and B can also rotate clockwise to another I_2^a, which is related to the intermediate structure in Fig. 3 and the final structure of Fig. 4 by the reflection with a mirror plane perpendicular to the [011] direction (see Fig. 4), namely, $\hat{x} \rightarrow \hat{x}$, $\hat{y} \rightarrow -\hat{y}$, $\hat{z} \rightarrow -\hat{z}$. This new I_2^a can perform the translation/rotation step in $[\bar{1}\bar{1}1]$,

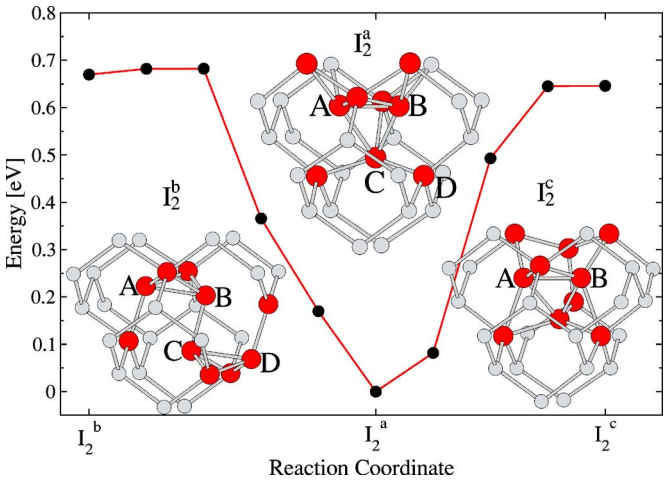

FIG. 5. (Color online) The transition path connecting the I_2^b, I_2^a, and I_2^c di-interstitial structures. The excited state di-interstitial I_2^b and I_2^c readily decay to the ground state di-interstitial I_2^a with almost zero barrier. The I_2^b di-interstitial is comprised of two dumbbell single interstitials, atoms A and B and atoms C and D, respectively, which are related by C_2 symmetry. The separation between the center of mass of each dumbbell estimates a 3.2 Å capture radius of two single interstitials.

[111], and $[\bar{1}1\bar{1}]$ directions with corresponding intermediate reorientation steps.

To summarize, the ground state di-interstitial I_2^a diffuses isotropically by a translation/rotation step along the four ⟨111⟩ bond directions with intermediate reorientation steps. The diffusion constant[25] is estimated by $D=\frac{4}{6}a^2\Gamma$. Here the diffusion jump rate, Γ, is given by the dominating translation/rotation step $\Gamma=11\ \mathrm{THz}\exp(-0.3\ \mathrm{eV}/k_BT)$ and the displacement during the translation/rotation step is $a=0.68$ Å. The effect of the intermediate reorientation steps on the diffusion is negligible due to their high rate and low barrier. The resulting diffusion constant is $D\approx 10^{-4}\exp(-0.3\ \mathrm{eV}/k_BT)\ \mathrm{cm}^2/\mathrm{s}$.

IV. PATHWAYS RELATING DIFFERENT DI-INTERSTITIALS

From earlier MD simulations[2] we extract the transition paths connecting I_2^a with I_2^b and I_2^c, respectively. These two transition paths are refined by the nudged-elastic band method.[16] Figure 5 shows the transition path connecting the three di-interstitials I_2^b, I_2^a, and I_2^c.

The transition path between I_2^b and I_2^a suggests that two single interstitials can form an I_2^a in a strong exothermic reaction. Notably, the I_2^b structure is a bound state of two *X*-site single interstitials given by the atom pairs A-B and C-D forming two dumbbells. The activation energy for the two bounded single interstitials to form I_2^a is about 10 meV, hence an I_2^b readily decays to an I_2^a at typical annealing temperatures. The center-of-mass separation between the dumbbells estimates a 3.2 Å capture radius[26] for two single interstitials to form an I_2^a.

The path between I_2^b and I_2^a provides another diffusion mechanism for I_2^a with a larger diffusion barrier of about 0.7 eV through the intermediate I_2^b structure. As shown in Fig. 5, the I_2^a with the ⟨110⟩-split dumbbell of atoms A and B transforms first to I_2^b. Since atoms A and B are equivalent to atoms C and D by C_2 symmetry, I_2^b can then transform to another I_2^a with a ⟨110⟩-split dumbbell of atoms C and D, completing the diffusion of I_2^a to a neighboring site.

Figure 5 also illustrates the transition between I_2^a and I_2^c. The I_2^c readily decays to I_2^a with nearly a zero barrier. The atoms A and B that form the ⟨110⟩-split dumbbell have a small displacement of 0.37 Å during the transition. The transition between I_2^a and I_2^c does not provide another diffusion path to neighboring sites for the I_2^a.

V. DISCUSSION

The low diffusion barrier of 0.3 eV for the ground state I_2^a suggests that I_2^a is a highly mobile structure. Given the 0.1–0.2 eV errors associated with the experimental measurements, this diffusion barrier is not inconsistent with the experimental value of 0.6 ± 0.2 eV.[5] The theoretical value for the diffusion barrier of single interstitials is about 0.3 eV.[15,27] This is consistent with a recent experiment[28] that observes the enhanced motion of single interstitials at 150 K. The di-interstitial I_2^a and single interstitials have similar diffusion barriers and are highly mobile structures. While the formation energy of di-interstitial is lower than for single interstitials on a per atom basis, it is much higher when considered on a total basis. Hence, in equilibrium di-interstitials are not present in any significant amounts in crystalline silicon. However, the large excess of interstitials during ion implantation[1] might induce a significant amount of di-interstitials. We believe that both di-interstitials and compact tri-interstitials[15] will have a significant amount of population in an ion-implanted silicon wafer due to their low formation energies on a per atom basis. As a result, the silicon single interstitials, di-interstitials and compact tri-interstitials might serve as mobile species that contribute to the enhanced diffusion of boron dopants.[1,29,30]

Figure 5 implies that the diffusion of single interstitials dominates the formation of the ground state di-interstitials. As mentioned before, the diffusion barrier of single interstitials is 0.3 eV, which is much larger than the barrier for two bound *X*-site single interstitials to form a ground state di-interstitial. Therefore, no additional energy is required for migrating single interstitials to form ground state di-interstitials. A reasonable inference is that the formation of ground state di-interstitials is dominated by the diffusion of single interstitials.

Here, the diffusion mechanisms for di-interstitials have been studied for the neutral charge state. On the other hand, positively charged states might lower the diffusion barrier of the I_2^a by about 0.1 eV.[8] However, the charged states will not change the conclusion that the di-interstitial I_2^a can diffuse along all possible ⟨111⟩ directions with translation/rotation and reorientation steps.

VI. CONCLUSION

We reveal the microscopic diffusion mechanism of the ground state di-interstitial I_2^a and show that di-interstitials can

perform isotropic diffusion along all possible ⟨111⟩ bond directions in the diamond lattice with intermediate reorientation steps. The translation/rotation step with a barrier of 0.3 eV and a prefactor of 11 THz dominates over the reorientation step with a barrier of 90 meV and a prefactor of 2300 THz. The dominating diffusion barrier of 0.3 eV for I_2^a is not inconsistent with the experimental value of 0.6 ± 0.2 eV.[5] In addition, the I_2^a structure can also diffuse to a neighboring site through an intermediate structure I_2^b, a bound state of two *X*-site single-interstitials, with a diffusion barrier of about 0.7 eV. The bound state of two *X*-site single-interstitials, I_2^b, can form a ground state I_2^a through a strong exothermic reaction. This suggests that (1) two migrating single interstitials can form a ground state di-interstitial without additional energy, and hence, (2) the diffusion of single interstitials dominates the formation process of di-interstitials.

ACKNOWLEDGMENTS

The work was supported in part by DOE-Basic Energy Sciences, Division of Materials Sciences (DE-FG02-99ER45795). Computing resources were provided by the Ohio Supercomputing Center.

*Electronic address: dyj@mps.ohio-state.edu

[1] D. J. Eaglesham, P. A. Stolk, H.-J. Grossmann, and J. M. Poate, Appl. Phys. Lett. **65**, 2305 (1994).
[2] D. A. Richie, J. Kim, S. A. Barr, K. R. A. Hazzard, R. Hennig, and J. W. Wilkins, Phys. Rev. Lett. **92**, 045501 (2004).
[3] J. Kim, J. W. Wilkins, F. S. Khan, and A. Canning, Phys. Rev. B **55**, 16186 (1992).
[4] S. Birner, J. Kim, D. A. Richie, J. W. Wilkins, A. F. Voter, and T. Lenosky, Solid State Commun. **120**, 279 (2001).
[5] Y. H. Lee, N. N. Gerasimenko, and J. W. Corbett, Phys. Rev. B **14**, 4506 (1976).
[6] Y. H. Lee, Appl. Phys. Lett. **73**, 1119 (1998).
[7] J. L. Benton, S. Libertino, P. Krighøj, D. J. Eaglesham, J. M. Poate, and S. Coffa, J. Appl. Phys. **82**, 120 (1997).
[8] J. Kim, F. Kirchhoff, W. G. Aulbur, J. W. Wilkins, F. S. Khan, and G. Kresse, Phys. Rev. Lett. **83**, 1990 (1999).
[9] G. H. Gilmer, T. D. de la Rubia, D. M. Stock, and M. Jaraiz, Nucl. Instrum. Methods Phys. Res. B **102**, 247 (1995).
[10] F. H. Stillinger and T. A. Weber, Phys. Rev. B **31**, 5262 (1985).
[11] M. Posselt, F. Gao, and D. Zwicker, Phys. Rev. B **71**, 245202 (2005).
[12] M. Cogoni, B. P. Uberuaga, A. F. Voter, and L. Colombo, Phys. Rev. B **71**, 121203(R) (2005).
[13] M. R. Sørensen and A. F. Voter, J. Chem. Phys. **112**, 9599 (2000).
[14] I. Kwon, R. Biswas, C. Z. Wang, K. M. Ho, and C. M. Soukoulis, Phys. Rev. B **49**, 7242 (1994).
[15] Y. A. Du, S. A. Barr, K. R. A. Hazzard, T. J. Lenosky, R. G. Hennig, and J. W. Wilkins, Phys. Rev. B **72**, 241306(R) (2005).
[16] H. Jónsson, G. Mills, and K. W. Jacobsen, in *Classical and Quantum Dynamics in Condensed Phase Simulations*, edited by B. J. Berne, G. Ciccotti, and D. F. Coker (World Scientific, Singapore, 1998), p. 385.
[17] G. Henkelman, B. P. Uberuaga, and H. Jónsson, J. Chem. Phys. **113**, 9901 (2000).
[18] G. Kresse and J. Hafner, Phys. Rev. B **47**, 558(R) (1993).
[19] G. Kresse and J. Furthmüller, Phys. Rev. B **54**, 11169 (1996).
[20] J. P. Perdew, in *Electronic Structure of Solids '91*, edited by P. Ziesche and H. Eschrig (Akademie Verlag, Berlin, 1991), p. 11.
[21] G. H. Vineyard, J. Phys. Chem. Solids **3**, 121 (1957).
[22] In NEB calculations, each image is relaxed until the perpendicular forces are less than 20 meV/Å.
[23] The silicon band gap of 0.72 eV within the generalized gradient approximation (Ref. 20) underestimates the actual band gap of 1.1 eV by 35%.
[24] In Ref. 8, Kim *et al.* call this translation/rotation step reorientation.
[25] A. R. Allnatt and A. B. Lidiard, *Atomic Transport in Solids* (Cambridge University Press, Cambridge, 1993), p. 272. In their Eq. (8.2.5), $z=4$, any $(s_{j,a})^2 = 1/3$.
[26] The formation energy of two separated single interstitials is about 1.3 eV higher than the bound state of two single interstitials I_2^b. Hence, we do not exclude the possibility that a larger capture radius may exist.
[27] G. M. Lopez and V. Fiorentini, Phys. Rev. B **69**, 155206 (2004).
[28] P. Partyka, Y. Zhong, K. Nordlund, R. S. Averback, I. M. Robinson, and P. Ehrhart, Phys. Rev. B **64**, 235207 (2001).
[29] P. A. Stolk, H.-J. Gossmann, D. J. Eaglesham, D. C. Jacobson, J. M. Poate, and H. S. Luftman, Appl. Phys. Lett. **66**, 568 (1995).
[30] L. H. Zhang, K. S. Jones, P. H. Chi, and D. S. Simons, Appl. Phys. Lett. **67**, 2025 (1995).